

Spectrally Constrained Global Analysis of Fluorescence Decays in Biomembrane Systems

M. M. G. Krishna and N. Periasamy¹

Chemical Physics Group, Tata Institute of Fundamental Research, Homi Bhabha Road, Colaba, Mumbai 400 005 India

Received May 2, 1997

Dynamic and steady-state fluorescence spectroscopic properties of a dye probe measured in a multi-component biological system are often required to be separated into the spectra and lifetimes of individual spectroscopically distinct species. The conventional method of obtaining decay-associated spectra fails when the lifetimes of the fluorophore in the membrane phase and in the aqueous phase are very close to each other. This paper describes a global analysis method which takes advantage of the known spectrum and lifetime of the dye in the aqueous phase. This method is used to identify the spectra for two fluorescent species (lifetimes, 0.84 and 1.97 ns) of the dye DODCI in EggPC vesicle membranes by keeping the spectrum and lifetime (0.68 ns) of the dye in the aqueous phase as fixed parameters. The structural identity of the two membrane-bound dye species was established by the effect of refractive index and/or viscosity of the aqueous medium on the lifetimes. © 1997 Academic Press

Key Words: global analysis; fluorescence; membrane; lifetime; DAS.

Fluorescence spectroscopic techniques are commonly used for the investigation of structure and dynamics in biological systems (1). Most of the biological systems are complex multicomponent systems consisting of an aqueous phase and one or more nonaqueous phases. Although fluorescent probes are often targeted to a specific phase, organelle, or compartment, it is not uncommon that the fluorophore (especially the polar or charged dyes) finds its way to the aqueous compartment which is the major compartment in all biological systems. Dynamic and steady-state fluorescence measurements of the whole system is a simple or convoluted sum of the spectral and dynamic properties of

the targeted component and the aqueous component. Separation of the fluorescence characteristics of the fluorophore in the targeted component is essential for the interpretation of the results.

A popular method of fluorescence analysis is to combine the dynamic time-resolved fluorescence data with the steady-state emission spectrum and obtain decay-associated spectra (DAS)² for the multicomponent system (1). Suppose that the fluorescence from a sample originates from n species of structurally distinct fluorophores in an m -component system and the spectra of the n species overlap. The fluorescence emission decays obtained at all emission wavelengths can be used to construct the spectrum of each species if the lifetimes of each species are sufficiently distinct from each other. The fluorescence decays are globally or individually fitted to the n -exponential function and the decay-associated spectra are constructed using

$$I_{\lambda,i} = I_{\lambda} \frac{\alpha_{\lambda,i} \tau_i}{\sum \alpha_{\lambda,j} \tau_j} = I_{\lambda} \frac{\alpha_{\lambda,i} \tau_i}{\tau_{av,\lambda}}, \quad [1]$$

where $I_{\lambda,i}$ is the intensity of the i th species with a lifetime τ_i , $\alpha_{\lambda,i}$ is the preexponent associated with the lifetime τ_i for the fluorescence decay collected at λ , I_{λ} is the steady-state intensity of the sample at λ , and $\tau_{av,\lambda}$ is the amplitude-weighted average lifetime. In practice, the decay-associated spectra can be constructed for a maximum of three to four species because of the limitations of fitting decay equations containing more than four exponentials.

The above method of decay-associated spectra fails even for $n = 3$ if the lifetimes of the dye in the aqueous phase and the nonaqueous phase are close to each other such that they are not resolvable. A method which takes advantage of the differences in the anisotropy

¹ To whom correspondence should be addressed. Fax: 091-22-215 2110. E-mail: peri@tifrvax.tifr.res.in.

² Abbreviations used: DAS, decay-associated spectra; ADAS, anisotropy DAS; IRF, instrument response function; MEM, maximum entropy method.

decay of the fluorophore in a multicomponent system has been described (2, 3) to obtain anisotropy decay-associated spectra (ADAS). We have developed a method which takes advantage of the fact that the spectrum of the dye in the aqueous phase is known. The spectrally constrained global analysis for determining decay-associated spectra has not been described in literature.

The method has been used for obtaining the decay associated spectra of DODCI in EggPC membrane. The spectra and lifetimes of two species of the dye in membrane were identified. Furthermore, the structures of the two membrane-bound dye species were established from the effect of refractive index and viscosity of the aqueous medium on the lifetimes.

EXPERIMENTAL

Methods and Materials

L- α -Phosphatidylcholine obtained from fresh egg yolk (EggPC; Sigma Chemical Co., USA), 3,3'-diethyloxadicarbocyanine iodide (DiOC₂ (5), DODCI; Exciton Inc., USA) were used in our fluorescence experiments without further purification. The EggPC vesicles were prepared by sonication (4) in buffer prepared in deionized water. The sonicated vesicles are of single bilayer with diameters in the range of 200–400 Å with nearly 70% of the vesicles having diameters \approx 300 Å. The buffer used was a mixture containing 10 mM CH₃COONa, 10 mM NaH₂PO₄, 10 mM 2-[N-morpholino]ethanesulfonic acid, and 150 mM NaCl for making solutions at pH 4.3. Sucrose (BDH, UK) was used to vary the refractive index (n_0) of the aqueous buffer from 1.334 to 1.413. Increasing the concentration of sucrose from 0 to 44.4% (w/w) increased the refractive index from 1.334 to 1.413 and the relative viscosity of the solution from 1 to 10.74. The refractive index measurements were done with Abbe's refractometer (Carl Zeiss Jena, Germany). The EggPC vesicles were prepared in seven different sucrose solutions ranging from 0 to 44.4% (w/w) so that the sucrose medium is present on either side of the bilayer. The buffer, vesicles, and sucrose solutions were tested to be free of fluorescence in the region of the dyes (550–750 nm). The typical concentration of the lipid used in these experiments was about 0.14 mM. The concentration of DODCI was \approx 0.25 μ M (dye:lipid ratio, 1:560). The dyes (dissolved in ethanol) were added to the vesicles and kept overnight before use.

The steady-state fluorescence and anisotropy measurements were made using either Shimadzu RF540 or SPEX Fluorolog 1681 T format spectrofluorophotometers. The time-resolved fluorescence measurements were made using a high-repetition-rate (800 kHz) picosecond dye laser (rhodamine 6G) coupled with a time-correlated single photon counting setup described elsewhere (5), currently using a microchannel plate photomultiplier

(Hamamatsu 2809). The sample is excited with vertically polarized light and the fluorescence decay is collected with emission polarizer kept at the magic angle (\approx 54.7°) with respect to the excitation polarizer. The instrument response function (IRF) was recorded using a nondairy creamer scattering solution. The full width at half-maximum of IRF is about 200 ps. Typical peak count in the emission decay for fluorescence intensity and anisotropy measurements is about 10,000 and the time per channel is 37.84 ps.

Fluorescence Decay Data Analysis

The experimentally measured fluorescence decay data is a convolution of the IRF and the intensity decay function (single or multiexponential). The popular method of deconvolution of individual fluorescence decay data is by the method of iterative reconvolution using the IRF and an assumed decay function whose parameters are improved in successive iterations. The iterative procedure for the optimization of the parameters (lifetimes, amplitudes, and shift) by the Levenberg–Marquardt algorithm has been described earlier (5–8). Global analysis for the simultaneous fitting of multiple fluorescence decays is a very useful technique for the accurate estimate of the parameters which are common to all the decay data sets (9). The main advantage of this method is the reduction in the number of free parameters to be optimized. Suppose there are n fluorescence decay data sets available for a sample (such as, for example, decays obtained at different emission wavelengths) for which the excited state decay is described by a three-exponential decay function, global analysis would treat the three lifetimes as common parameters for all the decay curves. The number of optimized parameters becomes ($4n + 3$) ($3n$ amplitudes, n shift parameters, and 3 lifetimes) instead of $7n$ in the case of individual analysis of the n decays. Further reduction in the parameters is possible if the amplitude relationship (that is, the spectrum for one component), if known, is incorporated. The method of spectrally constrained global analysis (described below) requires only ($3n + 4$) free parameters to be optimized; that is, a further reduction of ($n - 1$) parameters.

Let λ_p be either the peak wavelength or any other wavelength where the emission intensity is not equal to zero. Let $I_p(t)$ be the three exponential decay equation for the emission at λ_p ,

$$I_p(t) = \alpha_p e^{-t/\tau_1} + \beta_p e^{-t/\tau_2} + \gamma_p e^{-t/\tau_3}, \quad [2]$$

where α_p , β_p , and γ_p are the amplitudes for the three lifetimes, τ_1 , τ_2 , and τ_3 , respectively. Let $I_{s,p}$ be the steady-state spectral intensity of the sample at λ_p . The steady-state intensity $I_{s,p}$ is a sum of the intensities contributed by the three lifetime components. The intensity associated with τ_1 is given by

$$I_{s,p,\tau_1} = I_{s,p} \frac{\alpha_p \tau_1}{\alpha_p \tau_1 + \beta_p \tau_2 + \gamma_p \tau_3}. \quad [3]$$

Similarly, the intensity decay equation of the sample at any other wavelength λ_i is given as

$$I_i(t) = \alpha_i e^{-t/\tau_1} + \beta_i e^{-t/\tau_2} + \gamma_i e^{-t/\tau_3}, \quad [4]$$

and the steady-state intensity associated with τ_1 at λ_i is given by

$$I_{s,i,\tau_1} = I_{s,i} \frac{\alpha_i \tau_1}{\alpha_i \tau_1 + \beta_i \tau_2 + \gamma_i \tau_3}. \quad [5]$$

Let us assume that the steady-state spectrum associated with τ_1 is known (in our case, the dye in water) and the intensity at λ_p and λ_i are $I_{w,p}$ and $I_{w,i}$, respectively. Since the species (and spectrum) associated with τ_1 in membrane system and the dye in water are identical, the following equality holds.

$$\frac{I_{w,i}}{I_{w,p}} = \frac{I_{s,i,\tau_1}}{I_{s,p,\tau_1}} \quad [6]$$

Using Eqs. [3], [5], and [6], one gets

$$\frac{\alpha_i \tau_1}{\alpha_i \tau_1 + \beta_i \tau_2 + \gamma_i \tau_3} = \frac{\alpha_p \tau_1}{\alpha_p \tau_1 + \beta_p \tau_2 + \gamma_p \tau_3} x_i, \quad [7]$$

where x_i is a constant:

$$x_i = \frac{I_{w,i} I_{s,p}}{I_{w,p} I_{s,i}}. \quad [8]$$

Equation [7] can be resolved with respect to α_i ,

$$\alpha_i = \frac{\alpha_p x_i}{(1 - x_i) \alpha_p \tau_1 + \beta_p \tau_2 + \gamma_p \tau_3} (\beta_i \tau_2 + \gamma_i \tau_3). \quad [9]$$

Thus, the parameter α_i in Eq. [4] is not an independent parameter. α_p is the only amplitude parameter that has to be determined for τ_1 in the global analysis procedure for multiple decays collected at various emission wavelengths.

The Marquardt algorithm for the optimization of the values of free parameters requires the calculation of the convolution of integral $F(t)$ and partial derivatives of $F(t)$ with respect to the free parameters (7),

$$F_i(t) = \int_0^t G(s + \delta) I_i(t - s) ds, \quad [10]$$

where δ is the shift parameter, $G(t)$ is the instrument

response function, and $I_i(t)$ is the intensity decay function at λ_i as given by Eqs. [4] and [9]. Numerical calculation of $F_i(t)$ and its partial derivatives are performed using recursion relations (7). It may be noted that the amplitude parameter α_i is a function of all other parameters (α_p , β_p , γ_p , β_i , γ_i , τ_1 , τ_2 , and τ_3) and hence the recursion relations for the partial derivatives are different from those given by Grinvald and Steinberg (7). The recursion relations applicable for our method are given in the Appendix.

RESULTS AND DISCUSSION

The fluorescence decay of DODCI is single exponential in water ($\tau = 0.68$ ns in buffer) and in ethanol ($\tau = 1.07$ ns). A single exponential decay is a clear evidence that only one species is present in these samples. When the dye is bound to lipid vesicle membranes, the fluorescence decay is not single exponential. The number of distinct fluorescent species cannot be assumed even in this two component system. It is usual to fit fluorescence decays to two, three, or four exponential fits until good fit criteria are attained. An elegant method of analysis which does not assume the number of distinct species is the maximum entropy method (MEM) (10). The latter method gives distributions of lifetimes and the peaks of distributions are generally consistent with the discrete lifetimes. MEM is useful to limit the discrete exponential fit to the number of distribution (gaussian) peaks.

Figures 1A and 1B show the instrument response functions and the fluorescence decays of DODCI in vesicle membranes at two wavelengths (590 and 690 nm) and the results of analysis by MEM and discrete exponential analysis. The distribution of lifetimes is bimodal with peak positions at 0.66 and 1.78 ns for the fluorescence decay at 590 nm and 0.90 and 2.00 ns for the decay at 690 nm. The bimodal gaussian-like distribution of lifetimes suggests that a two exponential function would be adequate to fit the data. More positively, there is no evidence for the existence of a third lifetime component. The two lifetimes obtained in the two exponential fits of the decays at 590 nm are 0.65 and 1.75 ns and at 690 nm are 0.90 and 2.02 ns. In this case the two lifetimes are wavelength dependent. Figure 1C shows the distribution of weighted residuals for the two decays which indicate the absence of fast decay components. Figure 2 shows the variation of the two lifetimes with emission wavelength.

Variation of fluorescence lifetime(s) with emission wavelength is strong evidence that the two-species-two-lifetime model is not correct. It is therefore necessary to consider a three-exponential model. Since the fluorescence could be individually fitted adequately to two-exponential function, a three-exponential fit of individual decays is superfluous. However, a global anal-

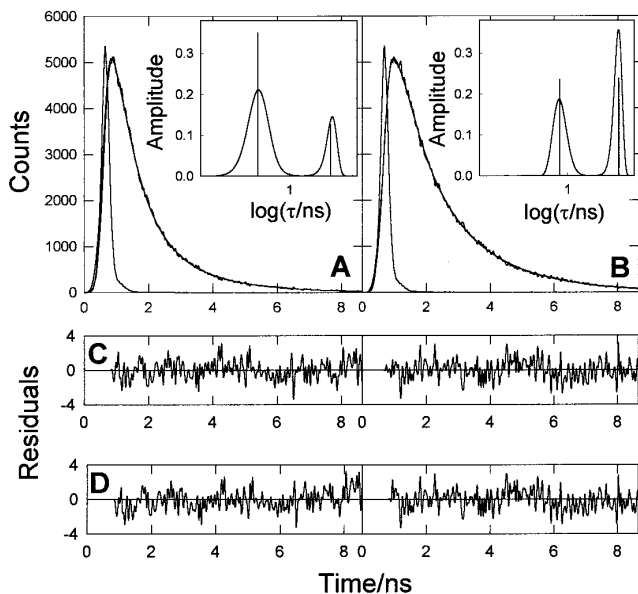


FIG. 1. Fluorescence decays of DODCI in EggPC vesicles for emission wavelengths at (A) 590 nm and (B) 690 nm. The instrument response functions at the excitation wavelength of 570 nm are also shown. The time per channel was 37.84 ps. The distribution of lifetimes obtained by MEM analysis ($\chi^2 = 1.02$ for 590 nm and $\chi^2 = 1.20$ for 690 nm) and discrete two exponential fit ($\chi^2 = 1.04$ for 590 nm and $\chi^2 = 1.17$ for 690 nm) are shown in the insets. C and D show the distribution of weighted residuals obtained in the case of two exponential fit where all the parameters are kept free and in the case of spectrally constrained global analysis respectively. The obtained mean lifetime values are (C) 590 nm: $\tau_{av} = 0.94$ ns, $\chi^2 = 1.04$; 690 nm: $\tau_{av} = 1.42$ ns, $\chi^2 = 1.17$; (D) 590 nm: $\tau_{av} = 0.96$ ns, $\chi^2 = 0.97$; 690 nm: $\tau_{av} = 1.42$ ns, $\chi^2 = 1.08$.

ysis of multiple fluorescence decays collected at all the emission wavelengths for three lifetimes which are common for all decays is still meaningful. The result of the global analysis gave the three lifetimes as 0.68 (fixed to that of the aqueous component), 0.74, and 1.90 ns for a $\chi^2_{global} = 1.09$. The variation in the amplitudes of the two short-lifetime components with the emission

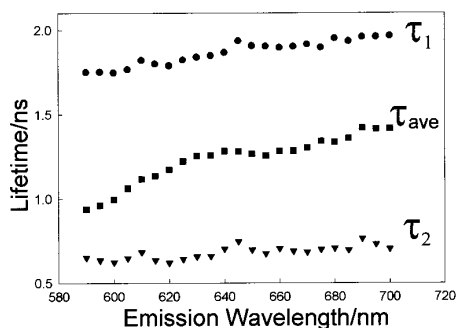


FIG. 2. Variation of the two lifetimes and the average lifetime obtained in the discrete two-exponential fit of the fluorescence decays of DODCI in EggPC vesicles with emission wavelength.

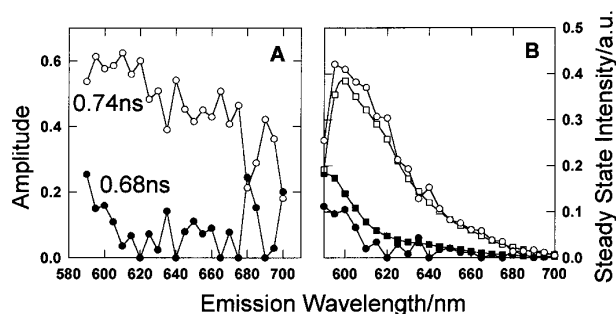


FIG. 3. (A) The amplitudes of the two short-lifetime components obtained in a global analysis of 23 fluorescence decays collected at different emission wavelengths. The unphysical oscillations in the amplitudes for lifetimes 0.68 and 0.74 ns are due to correlation effects due to the proximity of the lifetimes. (B) Decay-associated spectra for $\tau_1 = 0.68$ ns (aqueous component, solid symbols) and τ_2 (membrane-bound component, hollow symbols). The circles indicate the spectra obtained using the global analysis where the lifetime of DODCI in water is fixed. The squares indicate the spectra obtained with the spectrally constrained global analysis.

wavelength is shown in Fig. 3A and the decay-associated spectra for these components are shown in Fig. 3B. The amplitudes for the lifetime components 0.68 and 0.74 ns showed wild oscillations which are unphysical. The reason for the oscillation is presumably due to the closeness of the two lifetimes and as a result the values of the amplitudes for these two lifetimes become highly correlated. That is, a lower value of amplitude 1 is compensated by a higher value of amplitude 2. A straight forward global analysis is therefore not useful when two lifetimes are close to each other.

The solution to this problem lies in finding additional constraints in the global fitting strategy. In the problem of polar fluorescent probes such as DODCI (and similar potential sensing membrane cationic probes (11)) in membrane systems one of the lifetime components may be expected to be from the dye in the aqueous phase. The presence of a significant fraction of the dye in the aqueous phase could be confirmed by plotting the steady-state fluorescence anisotropy vs lipid concentration, as shown in Fig. 4, for DODCI and Nile red. In the case of Nile red, the dye is completely solubilized in the membrane even at a lipid concentration of 0.01 mg/ml and the steady-state anisotropy attains a constant value above this concentration. On the other hand, the binding of DODCI to the membrane is much less and, therefore, the steady-state anisotropy does not saturate below 0.05 mg/ml. For the experiments described in this work the lipid concentration used was 0.1 mg/ml and the steady-state anisotropy plot shows that the contribution of the dye present in the aqueous phase to the total fluorescence anisotropy is small. The discrete exponential analysis clearly shows that the short lifetime obtained at lower emission wavelengths matches with that of the dye in water. The emission

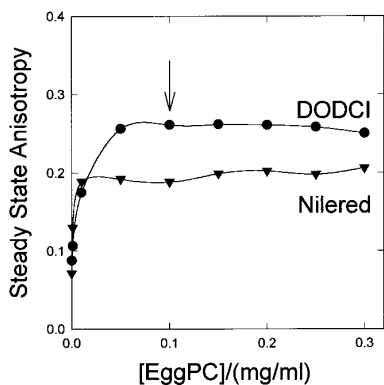


FIG. 4. Variation of steady-state anisotropy of DODCI and Nile red as a function of lipid concentration. The concentration of lipid used for vesicle samples is indicated by an arrow.

spectrum of DODCI in buffer shows that the emission maximum is 590 nm and there is negligible fluorescence at 690 nm. The fluorescence parameters (lifetime and spectrum) for the dye in the aqueous phase are known and these can be included in the spectrally constrained global analysis as described in the previous section.

The analysis of the fluorescence decays by the method described in this paper in which the spectrum and lifetime (0.68 ns) of DODCI in the aqueous phase were fixed gave the remaining two lifetimes as 0.84 and 1.97 ns. Figure 1D shows the distribution of weighted residuals for the two decays (Figs. 1A and 1B) obtained in the spectrally constrained global analysis. It may be noted that the decay-associated spectrum for the membrane-bound component (0.84 ns) is smooth in contrast to the spectrum associated with a 0.74-ns component obtained in global analysis in which only the lifetime of the aqueous component (0.68 ns) was fixed (Fig. 3B). Figure 5 shows the decay-associated spectra for the three lifetimes. The species with lifetimes of 0.84 and 1.97 ns are attributed to two structural variations of the dye in the membrane. The identity of the structures of DODCI in the membrane was investigated by the effect of sucrose in the aqueous solution on the lifetimes.

The refractive index and viscosity of the aqueous medium was changed by preparing sonicated vesicles in aqueous solutions of sucrose of concentration varying from 0 to 44.4% (w/w). The refractive index varied from 1.334 to 1.413 and the relative viscosity (η/η_0) was simultaneously increased from 1.0 to 10.74. The effect of the refractive index and/or viscosity on the three lifetimes are different. Figure 6 shows the variation of lifetimes with the sucrose concentration.

The fluorescence lifetime of DODCI in the aqueous phase increases from 0.68 to 1.20 ns with sucrose concentration. In homogeneous solutions, the radiative

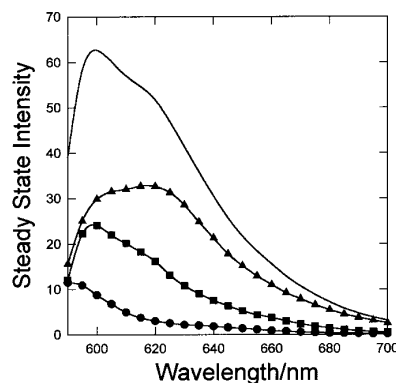


FIG. 5. The decay-associated spectra for the three lifetime components (\bullet , $\tau_w = 0.68$ ns; \blacksquare , $\tau_{\text{short}} = 0.84$ ns; and \blacktriangle , $\tau_{\text{long}} = 1.97$ ns, $\chi_{\text{global}}^2 = 1.03$) obtained by the spectrally constrained global analysis method described in this paper. The solid line is the steady-state spectrum of DODCI in Egg PC vesicles prepared in pH 4.3 buffer. See text for details.

rate of a fluorophore increases with the refractive index (square dependence) (12) and therefore the effect of refractive index ought to have decreased the fluorescence lifetime of DODCI, which is not the case. It is known that the nonradiative rate for cyanine dyes is strongly viscosity dependent (13). The increase in the

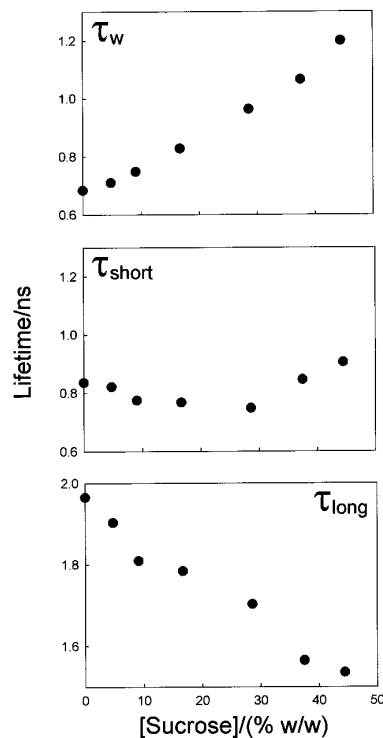


FIG. 6. The variation of the three lifetimes (associated with the three species of DODCI in the aqueous phase (τ_w) and membrane phase (τ_{short} and τ_{long})) with varying sucrose concentrations.

lifetime of DODCI in aqueous phase with sucrose concentrations is therefore entirely attributable to the viscosity effect.

The species with the lifetime of 0.84 ns shows a marginal decrease at low concentrations of sucrose and the lifetime increases marginally at higher concentrations. This trend is neither attributable solely to refractive index nor to the effect of viscosity. On the other hand, the species with the lifetime 1.97 ns decreases continuously with the sucrose concentration. The latter is a manifestation of refractive index effect on the radiative rate of DODCI (see below). These observations confirm that the species attributed to lifetimes 0.84 and 1.97 ns are bound to the membrane and that they are spectroscopically distinct species.

The effect of the refractive index of the aqueous medium on the radiative rate of a fluorophore bound to a thin layer was predicted (14, 15) to have strong dependence on the refractive index of the adjacent layer if the fluorophore is oriented normal to the thin layer. The refractive index effect is weak if the dye is oriented parallel to the surface. These predictions were found to be true in recent fluorescence lifetime experiments (15). Thus, the species with the lifetime 1.97 ns which shows strong dependence on refractive index is attributed to the dye oriented approximately perpendicular to the membrane surface. The species with the lifetime 0.84 ns shows a weak dependence on refractive index and thus it is attributed to the dye oriented parallel to the surface. The marginal viscosity effect at the high-sucrose region observed in the latter case suggests that the dye is probably on the surface of the bilayer membrane exposed to the aqueous phase.

The above experimental example illustrates the practical usefulness of the method of spectrally constrained global analysis in identifying the decay-associated spectra of the membrane-bound dye. The method will therefore be useful in most biological fluorescence studies if the probe (especially the water soluble one) is present or suspected to be present in the aqueous fraction.

CONCLUSIONS

The method of spectrally constrained global analysis described in this paper is useful for the analysis of dynamic fluorescence data in aqueous multicomponent fluorescent systems. The method is demonstrated in a case where the dye (DODCI) is distributed in the aqueous phase and the bilayer membrane phase. The two lifetimes associated with the membrane phase were assigned to the dye oriented parallel to the membrane surface and approximately perpendicular to the surface.

APPENDIX

The fluorescence response $F(t)$ at a given wavelength is a convolution of the instrument response function $G(t)$ and the intensity decay function $I(t)$ as given by Eq. [10]. In our case, the intensity decay function $I(t)$ is the three-exponential function as given by Eqs. [4] and [9]. The convolution integral can be written as (7)

$$F_m = \epsilon \sum_{j=1}^m G_j \sum_{k=1}^3 a_k \exp[-(m-j)\epsilon/\tau_k] \quad [11]$$

or

$$F_m = \sum_{k=1}^3 F_m^k \quad [12]$$

where F_m^k is the calculated fluorescence response in the m th channel due to the k th exponential component. a_k is the pre-exponential factor in the k th exponential. ϵ is the time duration of one channel.

For trapezoid integration, the following recursion relation can be used to calculate the F_m^k (7),

$$F_m^k = (F_{m-1}^k + 0.5\epsilon a_k G_{m-1}) \exp(-\epsilon/\tau_k) + 0.5\epsilon a_k G_m. \quad [13]$$

This equation results in the recursion relations between the partial derivatives of F_m^k with respect to the lifetimes

$$\begin{aligned} \frac{\partial F_m^l}{\partial \tau_1} &= \left[\frac{\partial F_{m-1}^l}{\partial \tau_1} + 0.5\epsilon G_{m-1} \frac{\partial a_1}{\partial \tau_1} + \frac{\epsilon}{\tau_1^2} [F_{m-1}^l + 0.5\epsilon a_1 G_{m-1}] \right] \\ &\quad \times \exp(-\epsilon/\tau_1) + 0.5\epsilon \frac{\partial a_1}{\partial \tau_1} G_m \\ \frac{\partial F_m^l}{\partial \tau_l} &= \left[\frac{\partial F_{m-1}^l}{\partial \tau_l} + 0.5\epsilon G_{m-1} \frac{\partial a_l}{\partial \tau_l} \right] \exp(-\epsilon/\tau_l) \\ &\quad + 0.5\epsilon \frac{\partial a_l}{\partial \tau_l} G_m; \text{ for } l = 2, 3 \\ \frac{\partial F_m^k}{\partial \tau_k} &= \left[\frac{\partial F_{m-1}^k}{\partial \tau_k} + \frac{\epsilon}{\tau_k^2} [F_{m-1}^k + 0.5\epsilon a_k G_{m-1}] \right] \\ &\quad \times \exp(-\epsilon/\tau_k); \text{ for } k = 2, 3 \\ \frac{\partial F_m^k}{\partial \tau_l} &= 0; \text{ for } l \neq k \neq 1. \end{aligned} \quad [14]$$

The partial derivatives of a_k with respect to the τ_1 , τ_2 , and τ_3 are nonzero only in the case of a_1 which are given below.

$$\begin{aligned}\frac{\partial a_1}{\partial \tau_1} &= -\frac{a_1(1-x_j)\alpha_p}{(1-x_j)\alpha_p\tau_1 + \beta_p\tau_2 + \gamma_p\tau_3} \\ \frac{\partial a_1}{\partial \tau_2} &= a_1 \left[\frac{\beta_i}{\beta_i\tau_2 + \gamma_i\tau_3} - \frac{\beta_p}{(1-x_j)\alpha_p\tau_1 + \beta_p\tau_2 + \gamma_p\tau_3} \right] \\ \frac{\partial a_1}{\partial \tau_3} &= a_1 \left[\frac{\gamma_i}{\beta_i\tau_2 + \gamma_i\tau_3} - \frac{\gamma_p}{(1-x_j)\alpha_p\tau_1 + \beta_p\tau_2 + \gamma_p\tau_3} \right]\end{aligned}\quad [15]$$

In the case of λ_p , the partial derivatives of F_m with the amplitudes α_p , β_p , and γ_p are

$$\begin{aligned}\frac{\partial F_m}{\partial \alpha_p} &= \frac{F_m^1}{\alpha_p} \\ \frac{\partial F_m}{\partial \beta_p} &= \frac{F_m^2}{\beta_p} \\ \frac{\partial F_m}{\partial \gamma_p} &= \frac{F_m^3}{\gamma_p},\end{aligned}\quad [16]$$

and at other wavelengths λ_i , the partial derivatives become

$$\begin{aligned}\frac{\partial F_m}{\partial \alpha_p} &= \frac{F_m^1(\beta_p\tau_2 + \gamma_p\tau_3)}{\alpha_p[(1-x_j)\alpha_p\tau_1 + \beta_p\tau_2 + \gamma_p\tau_3]} \\ \frac{\partial F_m}{\partial \beta_p} &= -\frac{F_m^1\tau_2}{[(1-x_j)\alpha_p\tau_1 + \beta_p\tau_2 + \gamma_p\tau_3]} \\ \frac{\partial F_m}{\partial \gamma_p} &= -\frac{F_m^1\tau_3}{[(1-x_j)\alpha_p\tau_1 + \beta_p\tau_2 + \gamma_p\tau_3]}\end{aligned}$$

$$\begin{aligned}\frac{\partial F_m}{\partial \beta_i} &= \frac{F_m^1\tau_2}{\beta_i\tau_2 + \gamma_i\tau_3} + \frac{F_m^2}{\beta_p} \\ \frac{\partial F_m}{\partial \gamma_i} &= \frac{F_m^1\tau_3}{\beta_i\tau_2 + \gamma_i\tau_3} + \frac{F_m^3}{\gamma_p}.\end{aligned}$$

ACKNOWLEDGMENT

The authors thank an anonymous referee for suggesting a significant improvement in the mathematical method described in this paper.

REFERENCES

1. Lakowicz, J. R. (1983) *in* Principles of Fluorescence Spectroscopy, Plenum, New York.
2. Knutson, J. R., Davenport, L., and Brand, L. (1986) *Biochemistry* **25**, 1805.
3. Davenport, L., Knutson, J. R., and Brand, L. (1986) *Biochemistry* **25**, 1811.
4. Krishnamoorthy, G. (1986) *Biochemistry* **25**, 6666.
5. Periasamy, N., Doraiswamy, S., Maiya, B. G., and Venkataraman, B. (1988) *J. Chem. Phys.* **88**, 1638.
6. Bevington, P. R., and Robinson, D. K. (1994) *in* Data Reduction and Error Analysis for the Physical Sciences, p. 161, McGraw-Hill, New York.
7. Grinvald, A., and Steinberg, I. Z. (1974) *Anal. Biochem.* **59**, 583.
8. O'Connor, D. V., and Philips, D. (1984) *in* Time Correlated Single Photon Counting, p. 174, Academic Press, London.
9. Knutson, J. R., Beechem, J. M., and Brand, L. (1983) *Chem. Phys. Lett.* **102**, 501.
10. Brochon, J. (1994) *in* Methods in Enzymology, Vol. 240, p. 262, Academic Press, London.
11. Haugland, R. P. (1996) *in* Handbook of Fluorescent Probes, p. 585, Molecular Probes Inc., Eugene, OR.
12. Birks, J. B. (1970) *in* Photophysics of Aromatic Molecules, p. 88, Wiley Interscience, London.
13. Aramendia, P. F., Negri, R. M., and San Roman, E. J. (1994) *J. Phys. Chem.* **98**, 3156.
14. Lukosz, W. (1980) *Phys. Rev. B* **22**, 3030.
15. Toptygin, D., and Brand, L. (1993) *Biophys. Chem.* **48**, 205.